engineering proceedings

MDPI

Proceeding Paper

Advanced Vibroacoustic Simulations Using Isogeometric Analysis †

Tommaso Landi [1,2,*,‡], Christophe Hoareau [2,‡], Jean-François Deü [2,‡], Roger Ohayon [2,‡] and Roberto Citarella [1,‡]

[1] Department of Industrial Engineering, University of Salerno, 84084 Fisciano, Italy; rcitarella@unisa.it
[2] Structural Mechanics and Coupled Systems Laboratory, Conservatoire National des Arts et Métiers, 75003 Paris, France; christophe.hoareau@lecnam.net (C.H.); jean-francois.deu@lecnam.fr (J.-F.D.); roger.ohayon@lecnam.net (R.O.)
* Correspondence: tlandi@unisa.it
† Presented at the 54th Conference of the Italian Scientific Society of Mechanical Engineering Design (AIAS 2025), Florence, Italy, 3–6 September 2025.
‡ These authors contributed equally to this work.

Abstract

This work presents a methodology for integrating Computer-Aided Design (CAD), specifically using Rhinoceros 6, with Isogeometric Analysis (IGA) for vibroacoustic simulations. Since CAD models typically provide only boundary representations, the 3D domain is reconstructed through an immersed IGA approach. The methodology is first illustrated in a 1D setting and then extended to a 3D case. The vibroacoustic coupling strategy is also described, enabling an efficient analysis of coupled fluid–structure vibrations. The proposed framework ensures direct CAD/CAE integration, thereby reducing preprocessing efforts.

Keywords: vibroacoustic; isogeometric analysis; immersed IGA; CAD/IGA integration

1. Introduction

Vibroacoustic problems, namely the interaction between elastic structures and surrounding fluids, play a central role in several engineering fields such as automotive, aerospace, and architectural acoustics [1]. Accurate modelling of these phenomena is crucial for predicting and controlling noise transmission and unwanted vibrations, which directly affect passenger comfort and structural performance [1,2]. Classical numerical techniques, such as the Finite Element Method (FEM) and the Boundary Element Method (BEM), are widely employed; however, they exhibit well-known limitations, particularly when large-scale problems lead to very high numbers of degrees of freedom [3].

Isogeometric Analysis (IGA) was introduced to address these challenges by exploiting the same spline functions, typically B-splines and Non-Uniform Rational B-Splines (NURBS), used in CAD systems to represent geometries, as well as to approximate the unknown physical fields [4]. This feature enables an exact description of the geometry, improved continuity of the basis functions, and superior convergence properties compared to traditional FEM [5]. In vibroacoustic applications, IGA has proven capable of providing more accurate predictions of eigenfrequencies, frequency responses, and fluid–structure coupling effects [5,6].

A major obstacle, however, remains the integration between CAD and numerical analysis. CAD models generally provide only a boundary representation (B-rep), whereas numerical simulations require a full volumetric description of the domain [7]. To overcome this issue, the immersed IGA technique has been developed, enabling the construction

Check for updates

Academic Editors: Nicola Bonora, Umberto Galietti, Luigi Bruno, Davide Castagnetti, Cristiana Del Prete, Mario Guagliano and Vigilio Fontanari

Published: 16 April 2026

Copyright: © 2026 by the authors. Licensee MDPI, Basel, Switzerland. This article is an open access article distributed under the terms and conditions of the Creative Commons Attribution (CC BY) license.

of three-dimensional IGA meshes directly from boundary representations [7–11]. This approach significantly reduces preprocessing costs, simplifies the handling of complex geometries, and preserves the accuracy and continuity advantages of IGA.

While this methodology has already been applied in the literature to the construction of 3D structural and optimization problems [12,13], the originality of the present work lies in the extraction of a 3D acoustic cavity via immersed IGA and its subsequent coupling with an external structure.

The proposed methodology is first illustrated through a 1D case to highlight the fundamental principles, and it is then extended to a 3D application, demonstrating its effectiveness and potential for engineering vibroacoustic applications.

2. Materials and Methods

2.1. Vibroacoustic Matrix Formulation

Let us introduce the vibroacoustic matrix formulation. The problem can be expressed in matrix form according to the following operators:

$$k(\delta u^h, u^h) = \delta \mathbf{u}^T \mathbb{K} \mathbf{u} \quad \Rightarrow \quad \mathbb{K} : \text{Structural Stiffness Matrix} \tag{1}$$

$$m(\delta u, u) = \delta \mathbf{u}^T \mathbb{M} \mathbf{u} \quad \Rightarrow \quad \mathbb{M} : \text{Structural Mass Matrix} \tag{2}$$

$$c(\delta u, p) = \delta \mathbf{u}^T \mathbb{C} \mathbf{p} \quad \Rightarrow \quad \mathbb{C} : \text{Coupling Matrix} \tag{3}$$

$$f(\delta u) = \delta \mathbf{u}^T \mathbf{f} \quad \Rightarrow \quad \mathbf{f} : \text{External Structural Force} \tag{4}$$

$$h(p, \delta p) = \delta \mathbf{p}^T \mathbb{H} \mathbf{p} \quad \Rightarrow \quad \mathbb{H} : \text{Acoustic Stiffness Matrix} \tag{5}$$

$$q(\delta p, p) = \delta \mathbf{p}^T \mathbb{Q} \mathbf{p} \quad \Rightarrow \quad \mathbb{Q} : \text{Acoustic Mass Matrix} \tag{6}$$

In the equations above, k denotes the virtual structural potential energy, m the virtual structural kinetic energy, c the virtual coupling energy on the structural side, and f the virtual external work. By analogy between the structure and the fluid domains, h and q are introduced as the virtual acoustic potential energy and the virtual acoustic kinetic energy, respectively. Moreover, the matrices $\mathbb{K}$ and $\mathbb{H}$ are positive semi-definite; the kernel of $\mathbb{K}$ has dimension six in 3D, while the kernel of $\mathbb{H}$ has dimension one. The matrix $\mathbb{M}$ is positive definite. Based on Equations (1)–(6), the operator can be written in discretized form as:

$$\left(\begin{bmatrix} \mathbb{K} & -\mathbb{C} \\ \mathbf{0} & \mathbb{H} \end{bmatrix} - \omega^2 \begin{bmatrix} \mathbb{M} & \mathbf{0} \\ \rho_f \mathbb{C}^T & \mathbb{Q} \end{bmatrix} \right) \begin{bmatrix} \mathbf{u} \\ \mathbf{p} \end{bmatrix} = \begin{bmatrix} \mathbf{f} \\ \mathbf{0} \end{bmatrix} \tag{7}$$

For further details, see [5,14].

2.2. 1D Immersed IGA

This section outlines the immersed IGA methodology. The objective is to demonstrate how a geometry can be reconstructed starting from its boundary definition only. CAD files generally provide a boundary representation of volumes, whereas numerical analyses, such as acoustic modal analyses in vibroacoustic problems, require a full volumetric description.

For clarity, the methodology is first presented in one dimension. The extension to 3D is straightforward, as it corresponds to a direct generalization of the 1D case.

A one-dimensional bar of length L is considered. The bar is discretized into n^0_{elem} elements at level 0 (initial arbitrary mesh), and the polynomial degree r is also defined. The element length is

$$L^0_{elem} = \frac{L}{n^0_{elem}} \tag{8}$$

and the corresponding number of basis functions is

$$n^0_{basis} = r + n^0_{elem} \tag{9}$$

At this stage, the displacement field $u^0(\xi)$ and the geometry $x^0(\xi)$ are approximated as follows:

$$u^0(\xi) = \sum_{i=1}^{n^0_{basis}} u_i N^0 * i, r(\xi)\ x^0(\xi) \qquad = \sum * i = 1^{n^0_{basis}} x_i N^0_{i,r}(\xi) \tag{10}$$

Consider the case in which the bar is cut at a point $x_{stop}(\xi_{stop})$, assumed to be located arbitrarily such that $x_{stop} \in [0, L]$ and $\xi_{stop} \in [0, 1]$. Figure 1 illustrates the bar, the corresponding basis functions, and the position of x_{stop}.

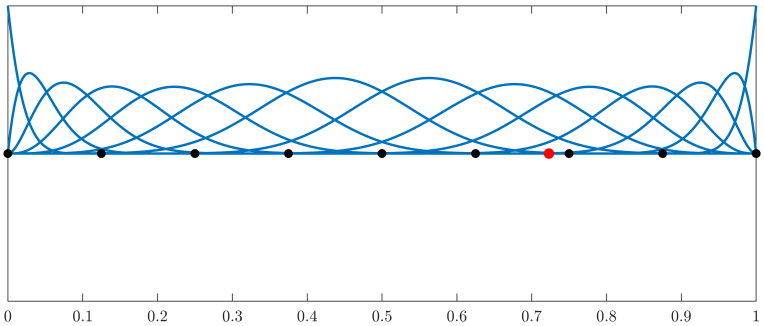


Figure 1. Basis functions with $r = 6$ and $n^0_{elem} = 8$. The cut point x_{stop} corresponds to the red marker. The black points correspond to the knot vector.

The procedure consists of identifying the following:

- The element containing ξ_{stop}, denoted e_{stop};
- The boundary effects (depending on r);
- The number of non-zero basis functions n^0_{remove} in that element;
- The remaining basis functions n^0_{keep}.

Once the basis functions to be replaced at level 0 are identified, they are substituted with a new set of functions obtained through h-refinement. The refinement is performed such that the number of elements at level 1, denoted n^1_{elem}, is twice that of level 0:

$$n^1_{elem} = 2 \times n^0_{elem} \quad \text{and} \quad L^1_{elem} = \frac{L}{n^1_{elem}} \tag{11}$$

The replaced basis functions from level 0, together with the new basis functions introduced at level 1, are illustrated in Figure 2.

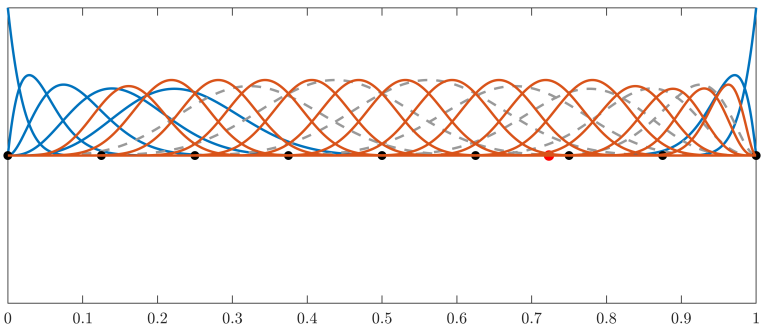


Figure 2. Kept basis functions of level 0 (in blue), replaced basis functions of level 0 (in gray), and new set of basis functions of level 1 (in orange).

The field discretization then becomes

$$u^1(\xi) = \sum_{i=1}^{n^0_{keep}} u_i N^0_{i,r}(\xi) + \sum_{i=1}^{n^1_{added}} u_i N^1_{i,r}(\xi) \tag{12}$$

This procedure can be repeated for l levels and it is called the Hierarchical B-Spline (HBs) approach.

A remark should be made regarding the edge effects. This aspect is discussed in Appendix A.

Afterward, it is necessary to identify the Gauss points that lie inside the domain of interest and those that fall outside of it. In this case, since the objective is to cut the bar at the red point, all Gauss points located to the right of this point are penalized by applying a weighting factor, ensuring that they do not influence the domain of interest. Furthermore, the degrees of freedom associated with the excluded portion of the domain are removed from the analysis.

The approach discussed in the one-dimensional case can be extended to three dimensions by applying the same procedure along the three spatial directions.

3. Results

This section presents the analysis of the results for two application examples.

The first example consists of a 1D bar of length L, which is cut at a random point x_{stop}, after which a modal analysis is performed. The results are compared with those obtained from an exact solution available for this case.

The second example deals with a 3D vibroacoustic problem. The acoustic cavity has a parallelepiped shape, and only its boundary is known. First, the 3D acoustic cavity is reconstructed using an immersed IGA approach, and an acoustic modal analysis is carried out. The results are then compared with those of an exact solution. Finally, the reconstructed acoustic cavity is coupled with a Kirchhoff–Love plate to evaluate the coupled vibroacoustic behaviour.

3.1. 1D Example

In this section, a tensile–compressive bar of length $L = 1$ is analyzed. The bar is cut at the point $x_{stop} = 0.7231$, after which a modal analysis is performed on the segmented bar. The obtained results are then compared with those from an exact solution. Figure 3 illustrates the problem under consideration.

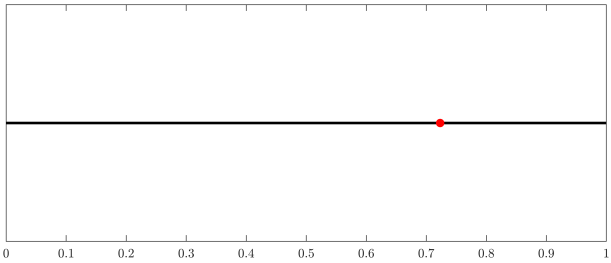


Figure 3. Traction–compression bar under investigation (in black). The cut location point is indicated by the red marker.

For the sake of simplicity, material parameters such as Young's modulus and density are set to unity. The adopted parameter values are summarized in Table 1.

Considering six levels (the initial level plus five refinement levels), the global basis functions considered are shown in Figure 4.

Table 1. Structural and geometrical parameter of the bar.

E [Pa]	ρ [$\frac{kg}{m^3}$]	L [m]	x_{stop} [m]	r [-]	n^0_{elem}
1.0	1.0	1.0	0.7231	6	8

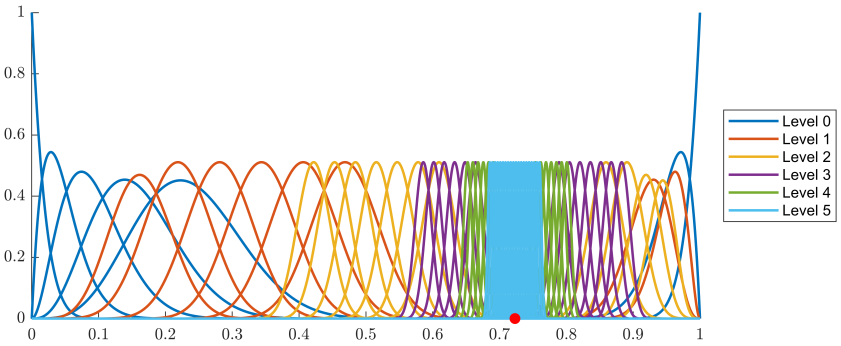


Figure 4. Global basis functions considered.

Figure 5 shows all the Gauss points of the considered problem. The Gauss points located outside the domain are penalized, while the integration is performed only on those lying inside the domain.

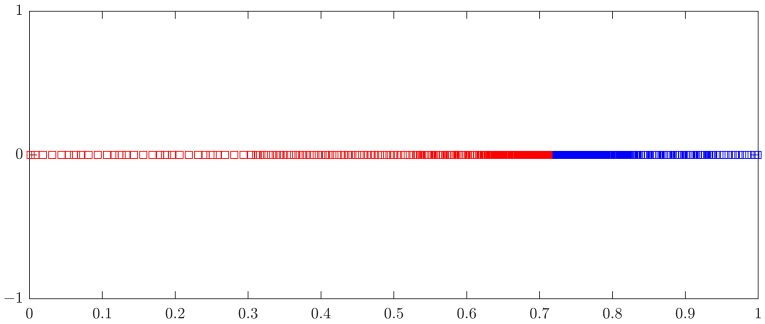


Figure 5. All Gauss points for the traction-compression bar application. Only the ones inside the domain (in red) are taken into account during the integration while the others (in blue) are penalized.

Figure 6 shows the first two numerical and analytical mode shapes, while Table 2 reports the computed frequency values along with the corresponding error respect to the exact solution.

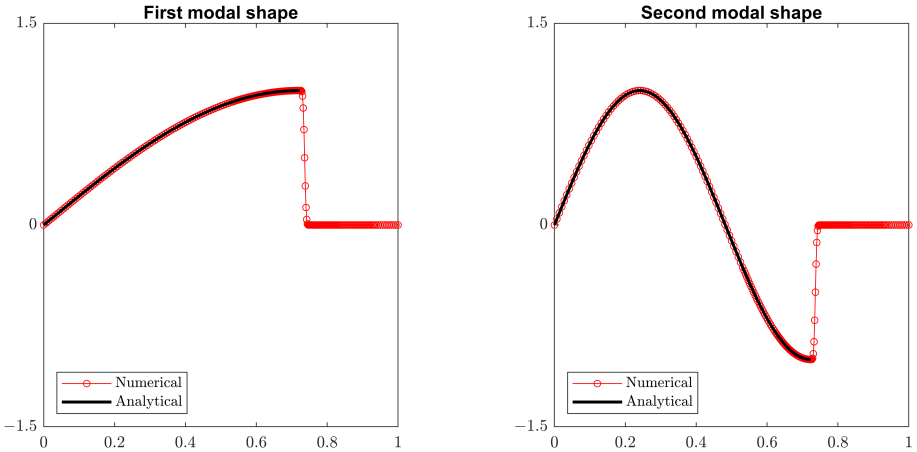


Figure 6. First two structural modal shapes. Numerical vs. analytical results.

Table 2. First five structural numerical and analytical frequencies and their corresponding percentage error.

f_{an} (Hz)	f_{num} (Hz)	Error (%)
0.346	0.346	0.03
1.037	1.037	0.03
1.729	1.729	0.03
2.420	2.420	0.03
3.112	3.112	0.03

3.2. 3D Example

This section is devoted to a three-dimensional example. Consider a geometry obtained from CAD software, as illustrated in Figure 7, which provides only the boundary representation of the domain. The dimensions of the geometry are $1 \times 1 \times 0.111111$. For this example, all parameters (Young's modulus, density, and sound speed) are set to 1, and three HB levels are constructed. The procedure to be followed consists of the following steps:

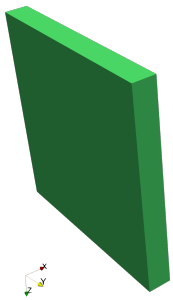


Figure 7. CAD geometry extracted from the CAD file.

- Immerse the geometry into an 3D IGA computational domain;
- Determine the number of refinement levels required to achieve a suitable approximation of the involved operators;
- Identify the basis functions to be retained at each level;
- Select only the Gauss integration points located inside the domain of interest, which will be used to perform the numerical integration.

The workflow of the process described above is illustrated in Figure 8.

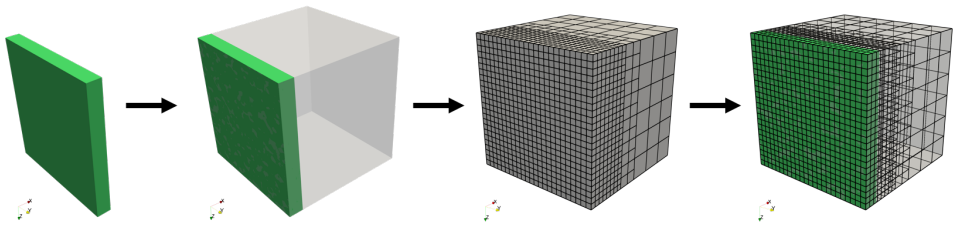


Figure 8. Workflow to be followed. Starting from the CAD geometry, it is embedded in an IGA cube; subsequently, a suitable number of levels are constructed for the analysis, and the CAD model is inserted within them.

Figure 9 shows the distribution of the Gauss points, highlighting those inside and outside the domain of interest. The numerical integration is carried out only on the internal points, while the external ones are penalized.

Table 3 reports the results of the first five numerical and analytical frequencies together with the corresponding percentage error. Furthermore, Figure 10 illustrates the first two numerical mode shapes.

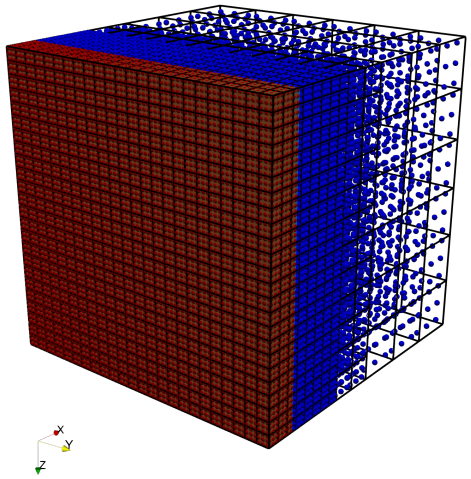


Figure 9. All Gauss points for the 3D acoustic cube application. Only the ones inside the domain (in red) are taken into account during the integration, while the others (in blue) are penalized.

Table 3. First acoustic numerical and analytical frequencies, as well as the corresponding percentage error.

f_{an} (Hz)	f_{num} (Hz)	Error (%)
0.500	0.500	0.001
0.707	0.707	0.001
1.000	1.000	0.002
1.118	1.118	0.010
1.414	1.414	0.011

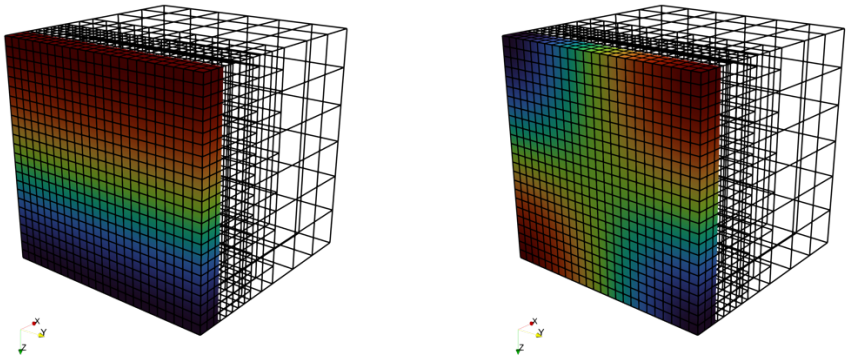


Figure 10. First two acoustic modal shapes.

3D Coupling

The coupling is performed at the 2D NURBS interface surface. The Gauss points in the two-dimensional structural parametric space are considered as integration points. In short, the integration over a 2D IGA surface involves two transformations. The main goal is to construct the coupling matrix:

$$c(p, \delta\mathbf{u}) = \int_{\Sigma_i} p\boldsymbol{n} \cdot \delta\mathbf{u}\, dS = \tag{13}$$

$$= \int_{\hat{\Sigma}_i} p^h(\boldsymbol{\xi}_f(\boldsymbol{\xi}_s))\boldsymbol{n} \cdot \delta\mathbf{u}^h(\boldsymbol{\xi}_s) J_1(\boldsymbol{\xi}_g) J_2(\boldsymbol{\xi}_s) d\hat{S} \tag{14}$$

$$\simeq \sum_{g=1}^{n_G} p^h(\boldsymbol{\xi}_f(\boldsymbol{\xi}_g))\boldsymbol{n} \cdot \delta\mathbf{u}^h(\boldsymbol{\xi}_g) J_1(\boldsymbol{\xi}_g) J_2(\boldsymbol{\xi}_g) w_g \tag{15}$$

$$\simeq \delta\mathbf{u}^T \left[\sum_{g=1}^{n_G} \mathbf{R}^T(\boldsymbol{\xi}_g)\mathbf{n}\mathbf{S}(\boldsymbol{\xi}_f(\boldsymbol{\xi}_g)) J_1(\boldsymbol{\xi}_g) J_2(\boldsymbol{\xi}_g) w_g \right] \mathbf{p} \tag{16}$$

At these points, it is necessary to evaluate the values of the NURBS basis functions on the structural side ($\mathbf{R}(\boldsymbol{\xi}_g)$), as well as the values of the HB functions on the fluid side (arising from the immersed IGA) ($\mathbf{S}(\boldsymbol{\xi}_f(\boldsymbol{\xi}_g))$). In the previous formula, J_1 and J_2 are the Jacobian of the two transformations.

To verify whether the coupling matrix has been properly constructed, a quasi-static analysis is performed on the problem illustrated in Figure 11. A displacement field equal to the structural mode shape itself is applied to the acoustic cavity. This procedure is repeated for the first four structural vibration modes, and a qualitative assessment is made to determine whether the resulting pressure field reproduces the displacement field.

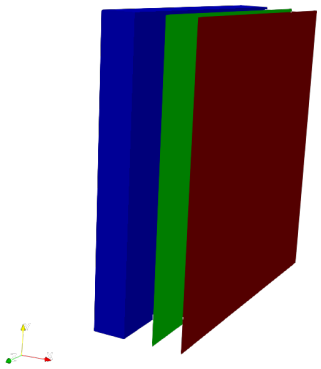


Figure 11. Vibroacoustic problem composed by an acoustic cavity (in blue), which comes from an Immersed IGA, a Kirchhoff–Love plate (in red), and their interface (in green).

The governing equation applied is

$$\mathbf{P} = \mathbb{H}^{+}\mathbb{C}\boldsymbol{\Phi}_{\mathbf{s}} \tag{17}$$

where $\mathbf{P}$ denotes the pressure field, $\mathbb{H}^{+}$ is the pseudo-inverse of the acoustic stiffness matrix, $\mathbb{C}$ is the coupling matrix, and $\boldsymbol{\Phi}_s$ represents the structural modal basis.

Figure 12 shows the first four structural modes and the corresponding acoustic response induced by these modes. The obtained pressure field is completely consistent with the structural modes.

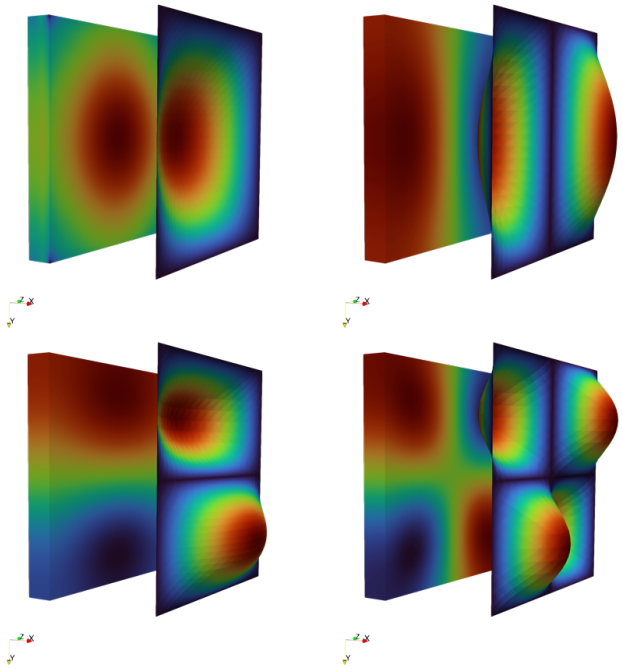


Figure 12. First four quasi-static fluid responses due to the structural mode.

4. Discussion and Conclusions

The results presented in this conference proceeding are very promising for future full integration between IGA and CAD. The outcomes obtained in both 1D and 3D cases are highly accurate with respect to exact solutions and can be readily extended to more complex geometries.

Future developments should focus on integrating the immersed IGA approach with complex geometries composed of multiple patches. Other possible research directions include investigating whether truncated B-splines offer actual advantages compared to hierarchical ones.

Author Contributions: Conceptualization, C.H. and T.L.; methodology, T.L., C.H., J.-F.D. and R.C.; software, T.L. and C.H.; validation, T.L. and C.H.; formal analysis, T.L.; investigation, T.L.; resources, T.L.; data curation, T.L.; writing—original draft preparation, T.L.; writing—review and editing, T.L., C.H., J.-F.D., R.O. and R.C.; visualization, T.L.; supervision, C.H., J.-F.D., R.O. and R.C. All authors have read and agreed to the published version of the manuscript.

Funding: This research received no external funding.

Institutional Review Board Statement: Not applicable.

Informed Consent Statement: Not applicable.

Data Availability Statement: No new data were created or analyzed in this study. Data sharing is not applicable to this article.

Conflicts of Interest: The authors declare no conflicts of interest.

Abbreviations

The following abbreviations are used in this manuscript:

CAD	Computer-Aided Design
IGA	Isogeometric Analysis
BEM	Boundary Element Method

FEM	Finite Element Method
NURBS	Not-Uniform Rational B-Splines
B-Rep	Boundary representation
HBs	Hierarchical B-Spline

Appendix A

The number of elements to split and the basis functions to be replaced depends on the edge effects. The number of elements to split is $[e_{stop} - r \leq e_{split} \leq e_{stop} + r]$. Indeed, the number of basis functions to be replaced changes and also depends on the current level.

- For level 0:
  - If $e_{split} \leq r$ and $e_{split} \geq (n^0_{elem} - r)$, the number of basis functions to be replaced is
    - On the right: $r - (n^{(0)}_{elem} - e_{split})$;
    - On the left: $(r - e_{split} + 1)$.
  - If $e_{split} \leq r$ and $e_{split} < (n^0_{elem} - r)$, then on the left, we need to take $(r - e_{split} + 1)$ basis functions.
  - If $e_{split} > r$ and $e_{split} \geq (n^0_{elem} - r)$, then on the right, we need to take $r - (n^0_{elem} - e_{split})$ basis functions.
- For levels higher than 0:
  - If $e_{split} \leq r$ and $e_{split} \geq n^l_{elem} - r$, then
    - On the right: $r - (n^l_{elem} - e_{split})$;
    - On the left: $r - e_{split} + 1$.
  - If $e_{split} \leq r$ and $e_{split} < (n^l_{elem} - r)$, then on the left, we need to take $(r - e_{split} + 1)$ basis functions.
  - If $e_{split} > r$ and $e_{split} \geq (n^l_{elem} - r)$, then on the right, we need to take $r - (n^0_{elem} - e_{split})$ basis functions.

  For more details, see [12,13].

References

1. Citarella, R.; Landi, T.; Caivano, L.; D'Errico, G.; Raffa, F.; Romano, M.; Armentani, E. Structural and Vibro-Acoustics Optimization of a Car Body Rear Part. *Appl. Sci.* **2023**, *13*, 3552. [CrossRef]
2. Armentani, E.; Sepe, R.; Parente, A.; Pirelli, M. Vibro-Acoustic Numerical Analysis for the Chain Cover of a Car Engine. *Appl. Sci.* **2017**, *7*, 610. [CrossRef]
3. Hughes, T.J.R.; Cottrell, J.A.; Bazilevs, Y. Isogeometric analysis: CAD, finite elements, NURBS, exact geometry and mesh refinement. *Comp. Methods Appl. Mech. Eng.* **2005**, *194*, 4135–4195. [CrossRef]
4. Austin Cottrell, J.; Hughes, R.; Bazilevs, Y. *Isogeometric Analysis: Toward Integration of CAD and FEA*, 1st ed.; Wiley: Hoboken, NJ, USA, 2009.
5. Landi, T.; Hoareau, C.; Deü, J.F.; Ohayon, R.; Citarella, R. Comparative vibroacoustic analyses: FEM vs. IGA. *Comput. Mech.* **2025**, *76*, 1027–1059. [CrossRef]
6. Song, X.; Jin, G.; Zhong, S.; Ye, T.; Chen, Y. Isogeometric modeling and vibro-acoustic analysis of flow-excited irregular cavity-plate-exterior space coupled system. *J. Sound Vib.* **2025**, *595*, 118712. [CrossRef]
7. Elbadry, Y.T.; Antolín, P.; Weeger, O. Immersed isogeometric analysis with boundary conformal quadrature for finite deformation elasticity. *Arch. Appl. Mech.* **2025**, *95*, 219. [CrossRef] [PubMed]
8. Teschemacher, T.; Bauer, A.M.; Oberbichler, T.; Breitenberger, M.; Rossi, R.; Wüchner, R.; Bletzinger, K.U. Realization of CAD-integrated shell simulation based on isogeometric B-Rep analysis. *Adv. Model. Simul. Eng. Sci.* **2018**, *5*, 19. [CrossRef]
9. Giannelli, C.; Jüttler, B; Speleers, H. THB-splines: The truncated basis for hierarchical splines. *Comput. Aided Geom. Des.* **2012**, *29*, 485–498. [CrossRef]
10. Schillinger, D.; Dedè, L.; Scott, M.A.; Evans, J.A.; Borden, M.J.; Rank, E.; Hughes, T.J.R.; An Isogeometric Design-through-Analysis Methodology Based on Adaptive Hierarchical Refinement of NURBS, Immersed Boundary Methods, and T-Spline CAD Surfaces. *Comput. Methods Appl. Mech. Engrg.* **2012**, *249–252*, 116–150. [CrossRef]

11. Garau, E.M.; Vázquez R. Algorithms for the Implementation of Adaptive Isogeometric Methods Using Hierarchical B-Splines. *Appl Num. Math.* **2018**, *123*, 58–87. [CrossRef]
12. Bornemann, P.B.; Cirak, F; A subdivision-based implementation of the hierarchical b-spline finite element method. *Comp. Method App. Mech. Engrg.* **2013**, *253*, 584–598. [CrossRef]
13. Xie, X.; Wang, S.; Xie, Q.; Liu, C.; Ren, Y.; Yang, A. Topology optimization using immersed isogeometric analysis and its software implementation. *Comput. Methods Appl. Mech. Engrg.* **2024**, *432*, 117374. [CrossRef]
14. Morand H.J.-P.; Ohayon, R. *Fluid-Structure Interaction: Applied Numerical Methods*, 1st ed.; Wiley: Hoboken, NJ, USA, 1995.

Disclaimer/Publisher's Note: The statements, opinions and data contained in all publications are solely those of the individual author(s) and contributor(s) and not of MDPI and/or the editor(s). MDPI and/or the editor(s) disclaim responsibility for any injury to people or property resulting from any ideas, methods, instructions or products referred to in the content.